

*Full Length Research Paper*

# Estimation of the compressive strength of high performance concrete with artificial neural networks

L. Acuña-Pinaud<sup>1\*</sup>, P. Espinoza-Haro<sup>1</sup>, I. Moromi-Nakata<sup>1</sup>, A. Torre-Carrillo<sup>1</sup> and F. García-Fernández<sup>2</sup>

<sup>1</sup>Faculty of Industrial and Systems Engineering, National University of Engineering, Av. Túpac Amaru, 210. Lima 25, Peru.

<sup>2</sup>Department of Forest Engineering, Polytechnic University of Madrid, Ciudad Universitaria S / N, 28040 Madrid, Spain.

Received 28 December, 2016; Accepted 10 August, 2017

High performance concrete is one of the most commonly used materials in non-standard building structures. Aside from the basic components used for its manufacture (water, cement, fine and coarse aggregates), other components such as fly ash, blast furnace slag and superplasticizers are incorporated. In the present study, two types of additives and two types of microsilica have been used. The proportions of all the elements involved in preparing concrete have an influence on its final strength. Artificial neural networks have been used to estimate the compressive strength of high performance concrete mixtures using the results obtained with 296 specimens corresponding to various fabrication parameters. The estimate given by the neural network was evaluated by measuring the correlation between network responses and the expected values, which are the strength values measured in the laboratory. The artificial neural network response obtained in the present work had a correlation of 92% with the expected values used for the training and 89% when predicting values for new data.

**Key words:** Artificial neuronal network, high performance concrete, compressive strength.

## INTRODUCTION

High performance concrete (HPC) is used for building structures subjected to high loads, in the construction of columns and beams of high-rise buildings, marine or military structures, security vaults, tunnels, bridges, among other applications. In all cases, a compression test is required after 28 days of immersion curing. The dynamics of HPC are very complex and the relationship between its strength and components is highly nonlinear. Several studies have shown that its strength depends not

only on the water-cement ratio, but also on all concrete ingredients: cement, fly ash, blast furnace slag, water, superplasticizer, age, coarse, and fine aggregates (Chou et al., 2011; Yeh, 1998, 2007). In Peru, there are practical experiences in the manufacture of HPC with additions of microsilica, mineral additives and chemicals, achieving 28-day strengths over 700 kg/cm<sup>2</sup> and reaching 1200 kg/cm<sup>2</sup> or more at 90 days (Rivva, 2008). In some studies of HPC with unsupervised neural networks, groups or

Corresponding author. E-mail: lacuna@uni.edu.pe.

Author(s) agree that this article remain permanently open access under the terms of the [Creative Commons Attribution License 4.0 International License](https://creativecommons.org/licenses/by/4.0/)

**Table 1.** Variables and statistics.

| S/N | Variable                         | MIN    | MAX     | STD   | MEAN   | CORREL |
|-----|----------------------------------|--------|---------|-------|--------|--------|
| 1   | Age (days)                       | 7.00   | 56.00   | 12.52 | 18.16  | 0.74   |
| 2   | Area (cm <sup>2</sup> )          | 80.40  | 83.50   | 0.52  | 82.08  | -0.24  |
| 3   | Additive                         | 1.00   | 2.00    | 0.34  | 1.86   | -0.53  |
| 4   | % Additive                       | 1.60   | 2.50    | 0.35  | 2.12   | 0.14   |
| 5   | Additive (kg/m <sup>3</sup> )    | 8.52   | 18.64   | 3.46  | 14.61  | 0.38   |
| 6   | % Microsilica                    | 5.00   | 10.00   | 2.08  | 7.24   | 0.13   |
| 7   | Microsilica (kg/m <sup>3</sup> ) | 26.63  | 74.56   | 16.68 | 49.88  | 0.30   |
| 8   | w/c ratio                        | 0.25   | 0.35    | 0.03  | 0.28   | -0.71  |
| 9   | Cement (kg/m <sup>3</sup> )      | 505.91 | 708.28  | 63.35 | 632.54 | 0.74   |
| 10  | Sand (kg/m <sup>3</sup> )        | 282.54 | 546.95  | 82.26 | 376.16 | -0.65  |
| 11  | Strength (kg/cm <sup>2</sup> )   | 565.00 | 1022.00 | 95.79 | 752.27 | 1.00   |

clusters of specimens have been found with common characteristics (Nataraja et al., 2006; Cal, 1995; Moromi et al., 2013). The published literature also contains large amount of information on the properties of concrete containing 10 to 30% fly ash.

### Database

In the present study, 296 concrete specimens (Figure 1) were manufactured with different types and amounts of cement, sand, aggregates, water and other compounds, in accordance with ASTM C 192/C 192M of 2000. The axial compression tests were performed (Figure 2) in accordance with ASTM C 39/C 39M of 2001, after various curing times.

The database (DB) recording the values of the manufacturing variables and the strength of the High-Performance Concrete (HPC) specimens (Table 1) was obtained by the Material Testing Laboratory of the Faculty of Civil Engineering of UNI. The original DB recorded 23 variables, including manufacturing variables and subsequent measurements, such as strength, load, test dates, among others. After preliminary data analysis, this original DB was reduced to another one including only 11 variables: 10 manufacturing variables and the compressive strength, as shown in Table 1, which also includes basic statistics and the correlation of each variable with the compressive strength (CORREL).

### Objective

The purpose of the study was to find a function of 10 variables evaluating the compressive strength of each specimen. But it is possible to build functions giving its approximate value using manufacturing data, through supervised artificial neural networks (ANN). The methods used in finding these approximate functions are based on the minimization of functions of many variables, in

particular functions that are sum of squares, known as least squares problems.

### MATERIALS AND METHODS

In addition to the materials normally used in manufacturing concrete, additives and microsilicas have also been used. Two brands of polycarboxylate-based liquid (polymers in aqueous solution) additives and two brands of microsilica (silica fume) have been used. Microsilica is a by-product of high-purity quartz reduction and its content of silicon dioxide (SiO<sub>2</sub>) is above 85% and in some brands, exceeds 93%. The type of additive used for each sample has been introduced as a qualitative variable. For proprietary reasons, no further details can be provided on these additives. The process for the manufacture of the mixture and the test specimens can be seen in Figures 5 and 6.

#### Additives

Additives are components added to the concrete mix immediately before or during mixing. The main reasons for their use are: (a) to reduce the cost of concrete structure, (b) to reach the desired concrete properties more effectively, (c) to maintain concrete quality during mixing, transportation, placement and curing in adverse weather conditions, and (d) to overcome emergencies during mixing, transportation, placement and curing.

#### Superplasticizer additives

Superplasticizer additives are premium water-reducing additives complying with ASTM C494-2013. They are used to give the concrete same properties as the usual water-reducing additives but carry out this task more efficiently. They correspond to ASTM C 494-2013 types F (water reducer) and G (water reducer and retarder). These additives can greatly reduce water demand and cement content and can produce concrete with low water/cement ratio, high strength and normal or high workability.

In the present investigation, percentages (p) of 1.5 to 2.5% of the cementing material have been used, depending on the ratio  $w / (c + p)$  to be used.

#### Microsilica

Microsilica, a by-product used as a pozzolan, results from the

**Table 2.** ANN input, matrix P.

| S/N | Variable                         | p <sub>1</sub> | p <sub>31</sub> | p <sub>70</sub> |
|-----|----------------------------------|----------------|-----------------|-----------------|
| 1   | Age (days)                       | 28.00          | 56.00           | 7.00            |
| 2   | Area (cm <sup>2</sup> )          | 81.70          | 82.50           | 81.60           |
| 3   | Additive                         | 1.00           | 1.00            | 2.00            |
| 4   | % Additive                       | 1.60           | 1.60            | 2.50            |
| 5   | Additive (kg/m <sup>3</sup> )    | 11.93          | 11.93           | 18.64           |
| 6   | % Microsilica                    | 5.00           | 5.00            | 7.50            |
| 7   | Microsilica (kg/m <sup>3</sup> ) | 37.28          | 37.28           | 55.92           |
| 8   | w/c ratio                        | 0.25           | 0.25            | 0.25            |
| 9   | Cement (kg/m <sup>3</sup> )      | 708.28         | 708.28          | 689.64          |
| 10  | Sand (kg/m <sup>3</sup> )        | 345.12         | 345.12          | 305.16          |

**Table 3.** Values of T for each P entry.

| T | Strength (kg/cm <sup>2</sup> ) | 836.00 | 969.00 | 758.00 |
|---|--------------------------------|--------|--------|--------|
|   |                                |        |        |        |

reduction of high purity quartz by coal in electric furnaces during the production of ferrosilicon. Microsilica comes out of the furnaces as vapor at about 2000°C (3620°F). On cooling, it is condensed and collected in large dust bags. Microsilica is then processed to remove impurities and control particle size. It is an extremely fine material with particles less than 1 µm in diameter and with an average diameter of about 0.1 µm, approximately one hundredth of the size of the average cement particle. The surface area of microsilica is about 20,000 m<sup>2</sup>/kg. Its specific gravity is generally 2.2 to 2.5, while the specific gravity of Portland cement is close to 3.15. The specific weight of microsilica varies from 130 to 430 kg/m<sup>3</sup>. It is sold as a powder but is most commonly found in the liquid form. It is used in amounts ranging from 5 to 10% of the total mass of the cementing material when a high degree of concrete impermeability and strength are necessary. The microsilica should conform to ASTM C 1240-2013. In the present work, percentages between 5 and 10% of the cementing material weight have been used for all the w / (c + p) ratios.

### Study of high strength concrete

In the following, MATLAB Version 7.10.0.499 (R2010a; licensed to Universidad Nacional de Ingeniería-UNI) has been used for numerical processing and the equations shown in the text uses its syntax. The Process of development of artificial neural network Backpropagation is seen in Figure 7

### Data entry

The DB was imported in MATLAB as two matrices: matrix P (10 rows, 296 columns) corresponding to the manufacturing variables of the test specimens; and matrix T (1 row, 296 components), corresponding to the compressive strengths. The columns of P are the input vectors of the ANN in Table 2 and are located in space R<sup>10</sup>. T contains the expected values and consists of a row array of 296 components.

### Classification of the columns of P and T for the simulation

The columns of matrix P and the components of T were numbered

from 1 to 296, as in Table 3. These values were separated into 5 subsets or disjoint classes, noted as Clas1, Clas2... Clas5. For example, Clas2 includes the values corresponding to the sequence of all the integers beginning with 2, to which 5 is added until one obtains a number smaller or equal to 296, such as: 2, 7, 12, ..., 287, 292. These groups of numbers are part of the equivalence classes of integers modulo 5.

The columns of P and the values of T corresponding to Clas5 were selected (any other class could have been taken) and these values were stored in matrices Pb and Tb respectively. These data were not used for network training, whereas the remainder of the data was stored in matrices Pa and Ta and used for network training.

### Standardization of data

The rows of Pa and Ta were transformed into others with means equal to zero and standard deviation equal to 1. This was achieved by doing: [pna, ps1] = mapstd(Pa); and [tna, ts] = mapstd(Ta). The Pa matrix was transformed into matrix pna, with the elements of the transformation corresponding to this process stored in file ps1. The mapstd function transformed the components (x) of each row of matrix Pa into another matrix, using the formula:

$$H(x) = (x - mc) / dc,$$

where mc and dc are respectively the mean and standard deviation of the row containing x. Similarly, the tna file was generated through the mapstd (Ta) transformation.

### Transformation of the dimension of pna columns

The second transformation is: [ptransa, ps2] = processpca (pna, 0.001). In this step, the pna matrix was transformed into ptransa and the elements of this transformation are found in the file ps2. The ps2 file contains a linear transformation (from R<sup>10</sup> to R<sup>6</sup>) transforming the pna columns (dimension 10) into others (dimension 6), without deleting any pna rows. This is possible because the covariance matrix of the transposed pna is a 10 × 10



Figure 1. Concrete specimens.

symmetric orthonormal matrix, and as such, has 10 real eigenvalues, of which 4 are of the order of  $10^{-14}$ , that is, very small. This led to the linear transformation mentioned earlier and explains the reduction in the dimension of the *pna* columns.

#### ANN training, validation and testing

To carry out these three phases, the *ptransa* columns were separated into three disjoint groups (using the equivalence classes of integers modulo 4), each group being as varied as possible within the column universe. The 1st and 3rd classes together (50%) were chosen for the training phase, the 2nd class (25%) for validation, and finally, the 4th class (25%) for testing.

#### Creation of the backpropagation ANN

This network, called RN1, consists of 4 layers with: 14 neurons in the first layer (this does not correspond to the number of rows, variables, of *ptransa*, which are 7; 12 neurons in the second; 10 in the third; and 1 neuron in the output layer, since the expected value *tna* is a  $1 \times 237$  matrix. The transfer functions are *tansig* (hyperbolic tangent) for the first three layers and *purelin* (identity) for the last layer. Trainlm was the implemented algorithm, using the Levenberg and Marquardt methods (Levenberg, 1944 and Marquardt, 1963).

## SIMULATION

#### RN1 response with training data

The result of interest is the correlation between RN1 response and *Ta*, the expected value. However, in order to clarify the process, this has been evaluated in another way. The response of RN1 to the *ptransa* matrix was simulated, that is, the response matrix:  $ra = \text{sim}(\text{RN1}, ptransa)$ . The original or real values of the response were obtained using the inverse function of *mapstd*:  $Ra = \text{mapstd}(\text{'reverse'}, ra, ts)$ , so that the matrix *Ra* was the response of RN1.

#### Correlation between *Ra* and *Ta*

The correlation between *Ra* and *Ta* was obtained with:  $[m, b, r] = \text{postreg}(Ra, Ta)$ , where in  $[m, b, r]$ , the values of *m* and *b* are respectively the slope and intersection with the y-axis of the regression line, and *r* is the linear correlation. The answers obtained are:  $ans = 0.8965, 79.6377, \text{ and } 0.92305$ .

#### Relationship between RN1 response *Ra*, the expected values *Ta*, and the errors *Ea*

The components of the *Ta* matrix were ordered from smallest to largest, together with the other two matrices. It can be seen from Figure 3 that the cloud of points representing *Ra* is very close to *Ta*.

#### Predictive capability of RN1

#### Network response with data *Pb* and expected value *Tb*

It is now possible to find out the compressive strengths predicted by RN1 for each column of *Pb* and to compare these with the actual strengths *Tb*. Following the same methodology as before, the first step consisted of normalizing the matrix *Pb*, thus obtaining the matrix *pnb*. Thereafter, the dimension of the columns of this matrix was reduced, using the same linear transformation defined by *ps2*. Thus, the matrix *ptransb* was obtained and the columns of this matrix were entered in RN1 for the simulation:  $rb = \text{sim}(\text{RN1}, ptransb)$ ;  $Rb = \text{mapstd}(\text{'reverse'}, rb, ts)$ . As previously, the actual values of RN1 response were obtained through the inverse of the *mapstd* function and stored in matrix *Rb*.

#### Correlation between *Rb* and *Tb*

The *postreg* function was used to find the level of correlation between *Rb* and *Tb*, making:  $[m, b, r] = \text{postreg}(Rb, Tb)$ . In  $[m, b, r]$ , the values of *m* and *b* are respectively the slope and intersection with the y-axis of the regression line, with *r* representing the linear correlation. These are:  $ans = 0.7914, 153.9445, \text{ and } 0.8973$ .

#### Graphs of *Tb*, *Pb* and *Eb*

Another way of interpreting the relationship between *Tb* and *Rb* is by plotting these two variables, after ordering the first matrix from smallest to largest, together with the other two matrices. It can be seen in Figure 4 that the cloud of points corresponding to *Rb* is located very close



**Figure 2.** Toni/Technik 3.000 KN testing equipment.

**Table 4.** Results obtained with different network architectures.

| ESTRUCTURE   | R    | R <sup>2</sup> | MSE   | RMSE  | #Weight+Biases |
|--------------|------|----------------|-------|-------|----------------|
| [14 12 10 1] | 0.92 | 0.85           | 1,313 | 36.24 | 419            |
| [7 14 1]     | 0.92 | 0.85           | 1,358 | 36.85 | 176            |
| [7 1]        | 0.89 | 0.78           | 1,913 | 43.74 | 57             |
| [1]          | 0.90 | 0.81           | 1,634 | 40.43 | 7              |

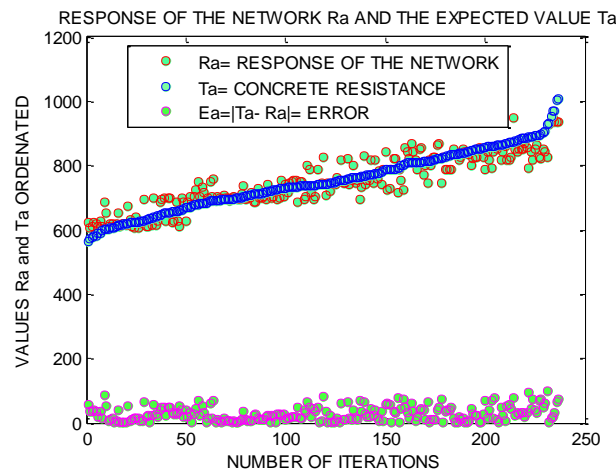


**Figure 3.** Comparison between network response Ra and expected values Ta, with training data. Ta: concrete strength / Ra: network response / Ea = |Ta - Ra|: error; Vertical: Ordered values of Ta and Ra; Horizontal: Rank.

to Tb.

**Other network architectures**

While using the same database and methodology as for RN1 with architecture [14 12 10 1], these tests were

conducted with three different network architectures, with the results as shown in Table 4.

**Conclusions**

RN1 network with 4 layers of 14, 12, 10 and 1 neurons,

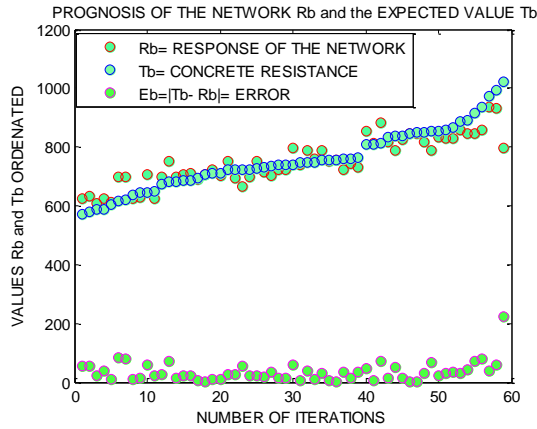


**Figure 4.** Comparison between network estimates  $R_b$  and expected values  $T_b$ , with test data.  $T_b$ : concrete strength /  $R_b$ : network estimate /  $E_b = |T_b - R_b|$ : error; Vertical: Ordered values of  $T_b$  and  $R_b$ ; Horizontal: Rank.

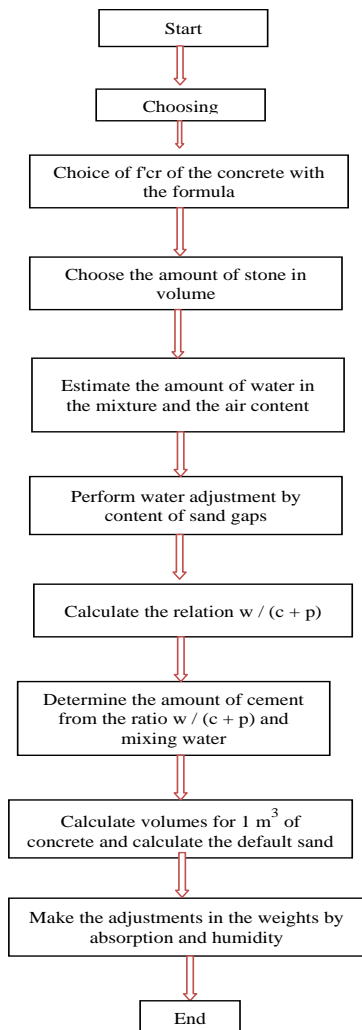


**Figure 5.** Flow diagram of the mix

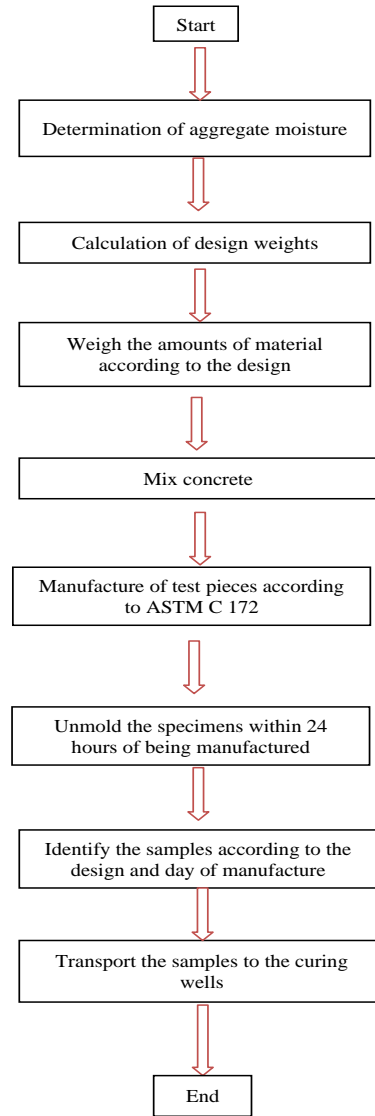


**Figure 6.** Flow chart of the sample manufacturing process.

respectively, obtained the highest correlation level ( $R = 0.92$ ;  $R^2 = 0.85$ ) and the lowest values for the mean squared errors. The predictive capacity of RN1 was tested using a set of 59 vectors not used for training. This test showed that RN1 provided satisfactory responses, with a correlation  $R = 0.90$ . The number of weights and biases of RN1 is 419, which is also the number of components of the variable  $x$  in the function  $e(x)$  and measures the quadratic mean of the difference between the RN1 response  $R_a$  and the expected value  $T_a$ . In spite of the number of variables, the RN1 response is highly correlated.

**CONFLICT OF INTERESTS**

The authors have not declared any conflict of interests.

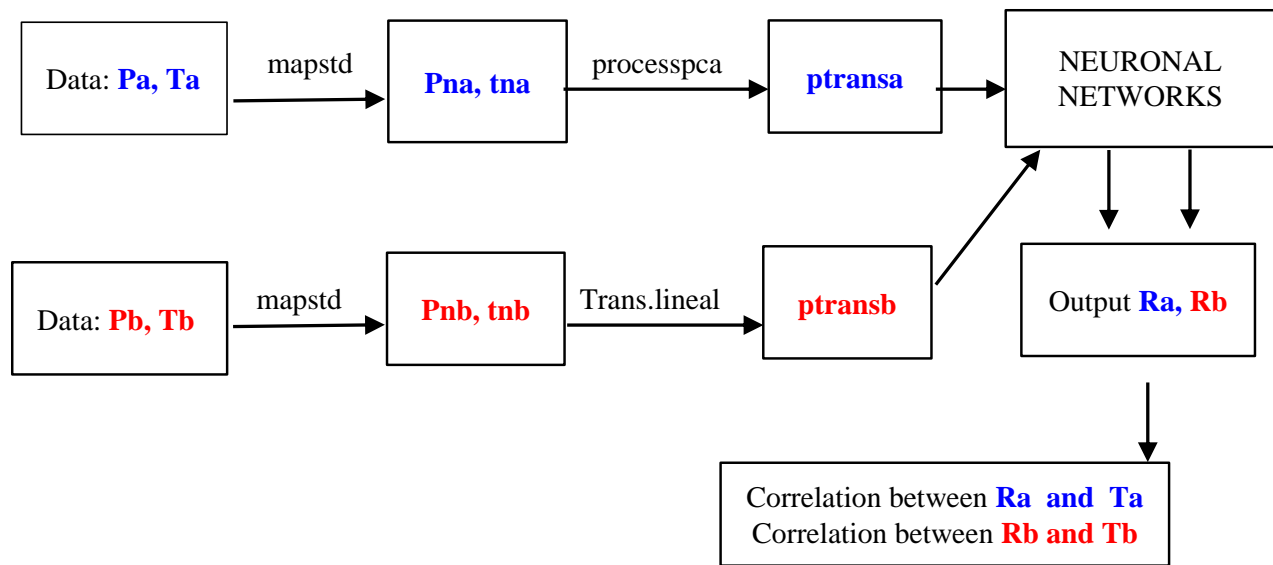


**Figure 7.** Process of development of artificial neural network Backpropagation.

## ACKNOWLEDGEMENT

The present work was carried out within the PIAP-1-P-676-13 Research Project funded by FINCyT within its 2013 Applied Research Program.

## REFERENCES

- Chou JS, Chiu CK, Farfoura M, Al Taharwa I (2011). Optimizing the Prediction Accuracy of Concrete Compressive Strength Based on a Comparison of Data-Mining Techniques. *J. Comp. Civil Eng.* 25(3):242-253.
- Rivva LE (2008). *Concreto de alta Resistencia*. Fondo Editorial Instituto Construcción y Gerencia. Lima Perú.
- Nataraja MC, Jayaram MA, Ravikumar CN (2006). Kohonen's feature maps for fly ash categorization. *Int. J. Neural Syst.* 16(06):457-466.
- Moromi NI, Torre CA, Acuña PL, García FF, Espinoza HP (2013). Self Organizing Maps estudio concreto alto rendimiento. <http://www.reddeperuanos.com/eci2015v/000selforganizationmaps.pdf>
- Yeh IC (1998). Modeling of strength of highperformance concrete using artificial neural networks. *Cem. Concr. Compos.* 28(12):1797-1808.
- Yeh IC (2007). Modeling slump flow of concrete using second-order regressions and artificial neural networks. *Cem. Concr. Compos.* 29:474-480.
- Cal Y (1995). Soil classification by neural network. *Adv. Eng. Softw.* 22(2):95-97.
- ASTM C 39 C 39 M (2001). The American Society for Testing Materials, Standard Test Method for Compressive Strength of Cylindrical Concrete Specimens. West Conshohocken PA. USA.
- ASTM C 192 C 192 M (2000) The American Society for Testing Materials Standard Practice for Making and Curing Concrete Test Specimens in the Laboratory. West Conshohocken PA. USA.
- Levenberg K (1944). A Method for the Solution of Certain Problems in Least Squares. *Quart. Appl. Math.* 2:164-168.
- Marquardt D (1963). An Algorithm for Least- Squares Estimation of Nonlinear Parameters. *J. Soc. Ind. Appl. Math.* 11(2):431-441.